PHYSICAL REVIEW D **95,** 114509 (2017)

Strange and charm quark spins from the anomalous Ward identity

Ming Gong (宫明),[1] Yi-Bo Yang (杨一玻),[2] Jian Liang (梁剑),[2] Andrei Alexandru,[3]
Terrence Draper,[2] and Keh-Fei Liu (劉克非)[2]
(χQCD Collaboration)

[1]*Institute of High Energy Physics, Chinese Academy of Science, Beijing 100049, China*
[2]*Department of Physics and Astronomy, University of Kentucky, Lexington, Kentucky 40506, USA*
[3]*Department of Physics, The George Washington University, Washington, D.C. 20052, USA*
(Received 18 November 2015; revised manuscript received 19 March 2017; published 22 June 2017)

We present a calculation of the strange and charm quark contributions to the nucleon spin from the anomalous Ward identity (AWI). This is performed with overlap valence quarks on $2+1$-flavor domain-wall fermion gauge configurations on a $24^3 \times 64$ lattice with lattice spacing $a^{-1} = 1.73$ GeV and the light sea mass at $m_\pi = 330$ MeV. To satisfy the AWI, the overlap fermion for the pseudoscalar density and the overlap Dirac operator for the topological density, which do not have multiplicative renormalization, are used to normalize the form factor of the local axial-vector current at finite q^2. For the charm quark, we find that the negative pseudoscalar term almost cancels the positive topological term. For the strange quark, the pseudoscalar term is less negative than that of the charm. By imposing the AWI, the strange $g_A(q^2)$ at $q^2 = 0$ is obtained by a global fit of the pseudoscalar and the topological form factors, together with $g_A(q^2)$ and the induced pseudoscalar form factor $h_A(q^2)$ at finite q^2. The chiral extrapolation to the physical pion mass gives $\Delta s + \Delta\bar{s} = -0.0403(44)(78)$.

DOI: 10.1103/PhysRevD.95.114509

I. INTRODUCTION

The quark spin content of the nucleon was found to be much smaller than that expected from the quark model by the polarized deep inelastic lepton-nucleon scattering experiments and the recent global analysis reveals that the total quark spin contributes only ∼25% to the proton spin [1].

In an attempt to understand the smallness of the quark spin contribution from first principles, several lattice QCD calculations [2,3] have been carried out since 1995 with the quenched approximation or with heavy dynamical fermions [4]. The most challenging part of the lattice calculation is that of the disconnected insertion of the nucleon three-point functions due to the quark loops. Recently, the strange quark spin $\Delta s + \Delta\bar{s}$ has been calculated with the axial-vector current on light dynamical fermion configurations [5–9] and it is found to be in the range from -0.02 to -0.03. This is about 4 to 5 times smaller in magnitude than that from a global fit of deep inelastic scattering (DIS) which gives $\Delta s + \Delta\bar{s} \approx -0.11$ [1] and a most recent analysis [10] including the JLab CLAS high precision data which finds it to be $-0.106(23)$ [11].

Such a discrepancy between the global fit of experiments and the lattice calculation of the quark spin from the axial-vector current is unsettling. It was emphasized some time ago that it is essential that a lattice calculation of the flavor-singlet axial-vector current be able to accommodate the triangle anomaly [12,13]. It was specifically suggested [12] to calculate the triangle anomaly from the vector-vector-axial (VVA) vertex and take it as the normalization condition for the axial-vector current in order to determine the normalization factor κ_A on the lattice. To address the discrepancy of the strange quark spin, we shall use the anomalous Ward identity (AWI) to provide the normalization and renormalization conditions to calculate the strange and charm quark spins in this work.

The structure of the rest of this paper is organized as follows. In Sec. II we introduce the theoretical framework of the quark spin calculation from AWI. In Sec. III the simulation details and results are provided. Conclusions are given in Sec. IV together with some outlooks.

II. FORMALISM

The anomalous Ward identity (AWI) usually refers to the flavor-singlet axial current $A^0_\mu = A^u_\mu + A^d_\mu + A^s_\mu$ in the flavor $SU(3)$ basis where there is a $U(1)$ anomaly term in the divergence of A^0_μ. However, the flavor $SU(3)$ is a global symmetry, AWI is satisfied for each flavor in the flavor basis through linear combinations of the flavor-octet axial current $A^8_\mu = A^u_\mu + A^d_\mu - 2A^s_\mu$ and isovector axial current $A^0_\mu = A^u_\mu - A^d_\mu$. For the case of the strange quark, its AWI can be obtained from the AWI for the A^0_μ and the WI for A^8_μ (N. B. there is no anomaly term in the WI for A^8_μ) through the combination $A^s_\mu \equiv \frac{1}{3}(A^0_\mu - A^8_\mu)$. Alternatively, the AWI can be derived for the strange by considering the infinitesimal local chiral transformation $\psi \to \psi + \delta_A\psi$, where $\delta_A\psi = i\epsilon(x)\gamma_5 T\psi$ with the 3×3 matrix in flavor space

$$T = \begin{pmatrix} 0 & 0 & 0 \\ 0 & 0 & 0 \\ 0 & 0 & 1 \end{pmatrix} = \frac{1}{3}(\mathbb{1} - \sqrt{3}\lambda^8),$$

where λ^8 is the eighth $SU(3)$ generator, gives a chiral transformation only for the strange.

For overlap fermions [14] which have chiral symmetry on the lattice via the Ginsparg-Wilson relation, the conserved flavor-singlet axial current is derived in [15]. Following the derivation with the above definition for the matrix T for the chiral transformation, it is straightforward to show that the following identity is satisfied for the strange axial-vector current:

$$\left\langle i\frac{\delta_A^s \mathcal{O}}{\delta\epsilon(x)}\right\rangle - \langle \mathcal{O}\partial_\mu^* A^s_{\mu,\mathrm{cons}}(x)\rangle + 2m_s\langle \mathcal{O}P^s(x)\rangle - 2i\langle \mathcal{O}q(x)\rangle = 0, \quad (1)$$

where ∂_μ^* is the forward lattice derivative. The expression of the conserved current for the strange quark $A^s_{\mu,\mathrm{con}}$ is given in Ref. [15] which involves a nonlocal kernel which is more involved to implement numerically than the local current. In this work we shall replace it with the local current $A^s_\mu = \bar{s}i\gamma_\mu\gamma_5(1-\frac{1}{2}D_{ov})s$, where D_{ov} is the massless overlap operator which is exponentially local with a falloff rate of about one lattice spacing [16]. The topological charge $q(x) = \mathrm{Tr}\gamma_5(\frac{1}{2}D_{ov}(x,x)-1)$ is derived in the Jacobian factor from the fermion determinant under the chiral transformation which is equal to $\frac{1}{16\pi^2}\mathrm{tr}_c G_{\mu\nu}\tilde{G}_{\mu\nu}(x)$ in the continuum [17], i.e.,

$$q(x) = \mathrm{Tr}\gamma_5\left(\frac{1}{2}D_{ov}(x,x)-1\right)\underset{a\to 0}{\to}\frac{1}{16\pi^2}\mathrm{tr}_c G_{\mu\nu}\tilde{G}_{\mu\nu}(x), \quad (2)$$

where Tr is the trace over both spin and color, while tr_c is the trace over color. For the strange quark spin, we shall consider the $\mathcal{O}$ in Eq. (1) to be the nucleon propagator, i.e.,

$$\mathcal{O} = \mathrm{Tr}\left[\Gamma_m\sum_{\vec{z}} e^{-i\vec{p}'\cdot\vec{z}}\chi(z,t)\sum_{\vec{y}} e^{-i\vec{p}\cdot\vec{y}}\bar{\chi}(y,0)\right], \quad (3)$$

where $\Gamma_m = (-i)\gamma_m\gamma_5(1+\gamma_4)/2$ is the spin polarized projection operator, and χ is the commonly used proton interpolation operator which involves two u and one d fields

$$\chi_\gamma(x) = \epsilon_{abc}\psi_\alpha^{\mathrm{T}(u)a}(x)(C\gamma_5)_{\alpha\beta}\psi_\beta^{(d)b}(x)\psi_\gamma^{(u)c}(x), \quad (4)$$

where the Latin letters denote the color index and the Greek letters denote the Dirac index and $C = \gamma_2\gamma_4$ is the charge conjugation matrix for the Pauli-Sakurai γ-matrix representation. In this case, the first term in Eq. (1) vanishes, since $\mathcal{O}$ does not involve strange quarks and hence no $\epsilon(x)$ dependence.

Following the standard calculation of off-forward nucleon matrix element [18,19], one considers the appropriate combination of the three-point function with the momentum projection of the current $\vec{q} = \vec{p'} - \vec{p}$ and the two-point functions to remove the kinematic dependence. The time separation between the nucleon source and the current insertion, and between the nucleon sink and the current insertion, is increased to the asymptotic region where the correlator is dominated by the nucleon. One arrives at the following unrenormalized AWI in nucleon matrix element for the strange quark

$$\langle p's|\partial_\mu\kappa_A A^s_\mu(q)|ps\rangle = \langle p's|2m_s P^s(q)|ps\rangle - \langle p's|2iq(q)|ps\rangle, \quad (5)$$

where $|ps\rangle$ is the nucleon state with momentum $\vec{p}$ and spin s. As we mentioned above, we shall replace the conserved axial-vector current $A^s_{\mu,\mathrm{cons}}$ with the local one $A^s_\mu = \bar{s}i\gamma_\mu\gamma_5(1-\frac{1}{2}D_{ov})s$. To compensate for the replacement, a normalization factor κ_A is introduced to make the AWI satisfied at finite cutoff. This is the only normalization factor needed since the pseudoscalar density P^s and the topological charge are the same as those in Eq. (1) [N. B. In the case of the disconnected insertion for the strange quark, the pseudoscalar density contributes through the quark loop. In this case, the P^s takes the form $P^s = \bar{s}i\gamma_5(1-\frac{1}{2}D_{ov})s$]. This lattice normalization factor is analogous to that introduced to make the chiral Ward identity satisfied for the local nonsinglet axial-vector current. In the literature, it is usually denoted as Z_A which is actually a finite renormalization with no logarithmic scale μ dependence. Following Ref. [20], we shall call it lattice normalization. Unlike the vector current and nonsinglet axial current, the flavor-singlet axial current has, in addition, a renormalization with anomalous dimension. We thus consider the renormalization on top of normalization as is done for the energy-momentum tensor in Ref. [19]. We will discuss the renormalization after we define the strange quark spin first.

The normalized strange quark spin in the nucleon $g_A^{s(N)} \equiv \kappa_A g_A^s = \Delta s + \Delta\bar{s}$, where g_A^s is the bare forward matrix element from the local axial-vector current

$$g_A^s s_\mu = \frac{\langle ps|A^s_\mu|ps\rangle}{\langle ps|ps\rangle}, \quad (6)$$

can be obtained by evaluating the right-hand (rhs) side of the AWI in Eq. (5) between the nucleon states in the forward limit, i.e.,

$$g_A^{s(N)} = \lim_{|\vec{q}|\to 0}\frac{i|\vec{s}|}{\vec{q}\cdot\vec{s}}\frac{\langle p's|2m_sP^s - 2iq|ps\rangle}{\langle p's|ps\rangle} = \frac{m_s}{m_N}g_P^s(0) + g_G(0), \quad (7)$$

where $g_P(0)$ and $g_G(0)$ are form factors at $q^2 = 0$ as defined in Eq. (7). The normalized charm spin $g_A^{c(N)} = \Delta c + \Delta\bar{c}$ is similarly defined. In this case, one can, in principle, calculate $g_P(q^2)$ and $g_G(q^2)$ at finite q^2 and extrapolate them to the $q^2 \to 0$ limit and this approach has been studied before [21,22]; however, the pseudoscalar density term was not included. Despite the fact that there is no massless pseudoscalar pole in the flavor-singlet case, it is shown that the contribution of the pseudoscalar density does not vanish at the massless limit [23,24]. Furthermore, there is a pion pole in the disconnected insertion of $g_P(q^2)$ to cancel that in the connected insertion to lead to η and η' poles [23,24]. Thus, the $g_P(q^2)$ and $g_G(q^2)$ form factors at small q^2 of the order of m_π^2 are essential for a reliable $q^2 \to 0$ extrapolation. Since the smallest $-q^2 = 0.21$ GeV^2 is larger than $m_\pi^2 = 0.11$ GeV^2 on the lattice we work on, a naive extrapolation of $q^2 \to 0$ in Eq. (7) may lead to a wrong result. To alleviate this concern, we shall consider instead, in this work, matching the $g_A(q^2)$ and the induced pseudoscalar form factor $h_A(q^2)$ from the left side of Eq. (5) and $g_P(q^2)$ and $g_G(q^2)$ from the right side at finite q^2 to determine the normalization constant κ_A as will be discussed later.

As far as renormalization is concerned, we note that in the continuum calculation [25], the renormalization constants of the quark mass and the pseudoscalar density cancel, i.e., $Z_m Z_P = 1$, and the renormalized topological charge term $-2iq$ has a mixing with the divergence of the axial current at one-loop in the form $\lambda\partial_\mu A_\mu^0$ where A_μ^0 is the flavor-singlet axial current and $\lambda = -(\frac{g_0^2}{4\pi^2})^2 \frac{3}{8} C_2(R) \frac{1}{\epsilon}$ with one of the g_0^2 coming from the definition of the topological charge. On the other hand, the renormalization of the divergence of axial-vector current occurs at the two-loop level involving a quark loop in the disconnected insertion which gives [25] the divergence of the renormalized strange axial-vector

$$\partial_\mu A_\mu^{s(R)} = \partial_\mu A_\mu^s + \lambda\partial_\mu A_\mu^0. \tag{8}$$

In the present work, we adopt the overlap fermion for the lattice calculation where $Z_m Z_P = 1$ and there is no multiplicative renormalization of the topological charge defined by the overlap operator in Eq. (2). After two-loop matching from the lattice to the $\overline{\text{MS}}$ scheme, the renormalized and normalized AWI equation at the scale μ is therefore

$$\begin{aligned}&\langle p's|\partial_\mu \kappa_A A_\mu^s + \gamma(\ln(\mu^2 a^2) + f)\partial_\mu A_\mu^0|ps\rangle \\ &\quad = \langle p's|2m_s P^s - 2iq + \gamma(\ln(\mu^2 a^2) + f')\partial_\mu A_\mu^0|ps\rangle,\end{aligned} \tag{9}$$

where $\gamma = -(\frac{g_0^2}{4\pi^2})^2 \frac{3}{8} C_2(R)$ is the anomalous dimension. We see that, modulo the possible different finite terms f and f' in the renormalization of A_μ^0 and the topological charge q [26], the anomalous dimension term on the left-hand side is the same as that on the rhs [25]. Thus, the two-loop renormalized AWI is the same as the *unrenormalized* AWI in Eq. (5).

Two loop renormalization on the lattice is quite involved, we plan to carry out the calculation of the lattice matching to the $\overline{\text{MS}}$ scheme nonperturbatively as is recently done in Ref. [9]. For the present work, we shall give an estimate of the renormalization correction. From the left side of Eq. (9), one finds the renormalized $g_A^{s(R)}$,

$$g_A^{s(R)} = g_A^{s(N)} + \delta g_A^s, \tag{10}$$

where $g_A^{s(N)} = \kappa_A g_A^s$ is the normalized g_A^s and

$$\delta g_A^s = \gamma(\ln(\mu^2 a^2) + f) g_A^0, \tag{11}$$

where g_A^0 is the flavor-singlet g_A.

To estimate the size of $\delta g_A^{s(R)}$ for renormalization and matching to the $\overline{\text{MS}}$ scheme at $\mu = 2$ GeV, we note that $g_0^2 = 2.82$ for the Iwasaki gauge action for domain-wall fermion (DWF) configurations, the lattice spacing $a^{-1} = 1.73$ GeV, and we assume f to be 10. In this case, $\gamma(\ln(\mu^2 a^2) + f) \sim 0.079$. Taking the experimental value of $g_A^0 = 0.25$ [1], we obtain $|\delta g_A^s| \sim 0.0066$. We shall take this as a part of the systematic error.

III. DETAILS

We use overlap fermions for the valence quarks in the nucleon propagator as well as for the quark loops on $2 + 1$ DWF $24^3 \times 64$ configurations with the light sea quark mass corresponding to a pion mass at 330 MeV [27]. Both DWF and overlap fermions have good chiral symmetry and it is shown that Δ_{mix}, which is a measure of mismatch in mixed action, is very small [28] and its effects on the nucleon properties have not been found to be discernible [29]. Since the $O(m^2 a^2)$ discretization errors are found to be small in the study of the charmonium spectrum and f_{D_s} [30], this allows us to compute the spin for the charm quark on this lattice. Moreover, the zero mode contributions to $2mP$ in the disconnected insertion (DI) and q in Eq. (7), which are finite volume artifacts, cancel when the overlap operator is used to define both of them.

The matrix element of the spin content can be obtained by calculating the ratio between the 3pt and the 2pt correlation functions:

$$\frac{\langle C(t_i, t_f)(O(t) - \langle O(t)\rangle)\rangle}{\langle C(t_i, t_f)\rangle}. \tag{12}$$

We adopt the sum method [31,32] where the insertion time of the $2mP$ quark loop and the topological charge q is summed between $t_i + 1$ and $t_f - 1$ where t_i/t_f is the

nucleon source/sink time. As a result, the summed ratio R $(\Delta t, q^2)$, where $\Delta t = t_f - t_i$, is linearly dependent on Δt and the slope is the matrix element of the spin content from $2mP$ or q,

$$\mathrm{R}(\Delta t, q^2) \underset{\Delta t \gg 1}{\longrightarrow} \mathrm{const} + \Delta t \langle p's|O|ps\rangle \frac{i|\vec{s}|}{\vec{q}\cdot\vec{s}}, \qquad (13)$$

from which we can obtain $m/m_N g_P(q^2)$ and $g_G(q^2)$ as functions of the momentum transfer squared q^2.

As explained in detail in [29,33], we adopt the Z_3-noise grid smeared source for the quark propagators of the nucleon, with support on some uniformly spaced smeared grid points on a time slice, and low-mode substitution which improves the signal-to-noise ratio substantially. For the $24^3 \times 64$ lattice, we place two smeared sources in each spatial direction, eight in total, each with a Gaussian smearing radius of about four lattice spacings, and have seen a gain of roughly 6 times of statistics in the effective nucleon mass as compared to that of one smeared source. In view of the fact that the useful time window for the nucleon correlator $C(t)$ is less than 14 and we have $T = 64$ slices in time, we put two grid sources at $t = 0$ and 32 simultaneously to gain more statistics from one inversion. Thus, our grid has the pattern of (2,2,2,2) with two smeared grid sources in each of the space and time directions. We shift the original grid along the temporal direction to cover all time slices, and it requires 32 inversions for each configuration.

Since both the strange and charm contributions result from the disconnected insertions (DI), the calculation involves the product of the nucleon propagator and the quark loop. For the quark loop, we employ the low mode average algorithm which entails an exact loop calculation for the low eigenmodes of the overlap operator over all space time points on the lattice. On the other hand, the high modes of the quark loops are estimated with 4D $Z(4)$ noise grid sources. The spatial interval of the grid is four lattice spacings and the temporal interval is two lattice spacings. We also construct another grid generated by shifting the original grid by one lattice spacing along the temporal direction, so that all time slices are covered. The two grids are further diluted according to the 4D even-odd sites on the grids. This scheme requires four inversions for each $Z(4)$ noise set and we have eight noise sets for one configuration, therefore we have 32 inversions in total for each configuration.

The AWI splits the divergence of the axial current into two parts, i.e., $2mP$ and q, and the two parts reveal different aspects of the physics contribution. The pseudoscalar part is low-mode dominated for light quarks, where the lowest 200 pairs of overlap eigenvectors contribute more than 90% of the vacuum value for the very light quarks and ~70% for the strange [29]. The overlap Dirac operator $D_{ov}(x, y)$ in the definition of the topological term in Eq. (2) is exponentially local with an exponential falloff rate of about one lattice spacing [16]. Thus, the anomaly part, being local, captures the high-mode contribution of the divergence of the axial-vector current.

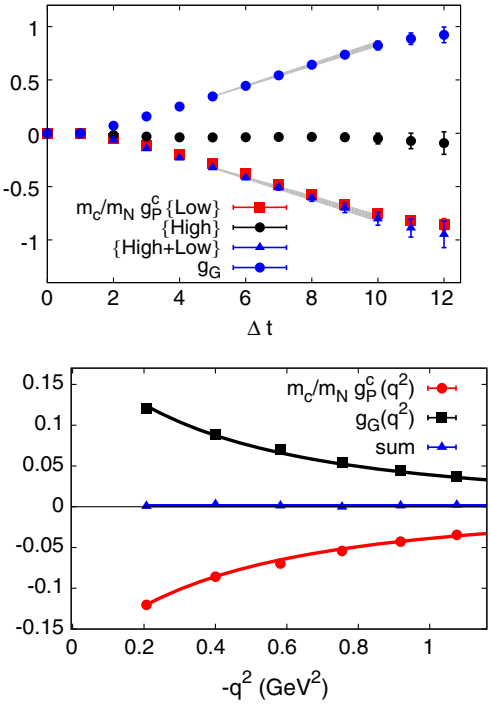

FIG. 1. (Upper panel) The summed ratio of three-point and two-point correlators as a function of Δt where the slopes are the contributions from $2mP$ and q at $|\vec{q}| = 2\pi/La$ in the DI for the charm quark in Eq. (13). The red squares and the black points are the low- and high-mode contributions respectively. The blue triangles with error band are the total. The valence quark in the nucleon is the same as that of the light sea at $m_\pi = 330$ MeV. The similar summed ratio for the contribution from the topological charge q is plotted as blue points whose slope gives $g_G(q^2)$. (Lower panel) The $2mP$ contribution $m/m_N g_P^c(q^2)$ and the anomaly contribution $g_G(q^2)$ are plotted as a function of $-q^2$.

We first show the summed ratio in Eq. (13) for the charm quark as a function of Δt for the case with lowest momentum transfer, i.e., $|\vec{q}| = 2\pi/La = 0.469$ GeV (corresponding to $q^2 = -0.207$ GeV^2) in the upper panel of Fig. 1. The contributions from the low modes and high modes for $\frac{m_c}{m_N} g_P^c(q^2)$ at this $|\vec{q}|$, which are coded in the slopes, are shown separately. They are from the case where the valence quark in the nucleon and that of the light sea have the same mass which correspond to $m_\pi = 330$ MeV (the so-called *unitary point*). It is clear from the upper panel of Fig. 1 that low modes dominate the contributions. Even though the low modes contribute only ~20% in the charm quark loop itself [29], they become dominant when correlated with the nucleon. On the other hand, the $g_G(q^2)$ from the slope at this $|\vec{q}|$ is large and positive. The errors for $\frac{m_c}{m_N} g_P^c$ and g_G are 6% and 4%, respectively.

In the lower panel of Fig. 1, we give the results for the charm quark ($m_c^R a = 0.73$) which is determined from a global analysis of the charm mass [30]. The pseudoscalar

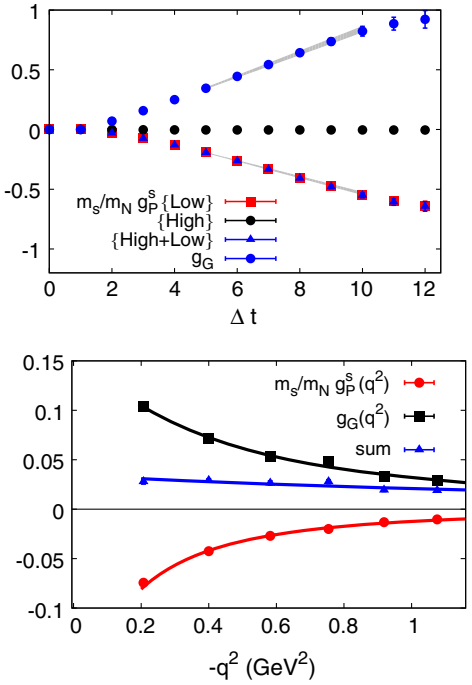

FIG. 2. The same as in Fig. 1 but for the strange quark.

density term (red points) and the topological charge density term (black squares) are plotted as a function of $-q^2$. We see that the pseudoscalar contribution is large, due to the large charm mass, and negative while the anomaly is large and positive. The lines are fits with a dipole form just to guide the eye. When they are added together (blue triangles in the figure), they are very close to zero, with small statistical errors, over the whole range of $-q^2$. Thus, when extrapolated to $q^2 = 0$ with a constant, we obtain $\Delta c + \Delta\bar{c} = -9.5(2.8) \times 10^{-4}$ at the unitary point. When extrapolated to the physical pion mass, $\Delta c + \Delta\bar{c} = -2.7(2.8) \times 10^{-4}$, which shows that the charm hardly contributes anything, if at all, to the proton spin due to the cancellation between the pseudoscalar term and the topological term. It is known [34] that the leading term in the heavy quark expansion of the quark loop of the pseudoscalar density, i.e., mP, is the topological charge $\frac{i}{16\pi^2}\mathrm{tr}_c G_{\mu\nu}\tilde{G}_{\mu\nu}$ which cancels the contribution from the topological term in the AWI. To the extent that the charm is heavy enough such that the $\mathcal{O}(1/m^2)$ correction is small, the present results of cancellation can be taken as a cross-check of the validity of our numerical estimate of the DI calculation of the quark loop as well as the anomaly contribution. The mixing for the heavy quark loops from the other favors are also highly suppressed and negligible at the present stage.

Next, we consider the case with the strange quark ($m_s a = 0.063$) for this lattice, which is again determined from the global fit for the strange quark mass based on fitting of D_s and D_s^* [30]. Similarly to Fig. 1, $\frac{m_s}{m_N} g_P^s(q^2)$ and $g_G(q^2)$ are plotted in Fig. 2 for the unitary case where the valence quarks in the nucleon and the light sea quarks have the same mass at $m_\pi = 330$ MeV. We see in the upper panel that the low modes completely dominate the $2m_s P^s$ contribution as in the case of charm. The anomaly is the same for all flavors. In the lower panel, it is shown that the contribution from $2m_s P^s$ is only slightly smaller than that of the charm. This is due to the fact that even though the strange quark mass is about 12.5 times smaller than that of the charm [30], its pseudoscalar matrix element is much larger than that of the charm. Since the anomaly is the same for the strange and the charm, the sum of $\frac{m_s}{m_N} g_P^s(q^2)$ and $g_G(q^2)$, shown in the lower panel, is slightly positive in the range of $-q^2$ as plotted.

Since our smallest $q^2 = -0.207$ GeV^2 is larger than m_π^2 which should be present as the pion pole on the right-hand side of the DI of AWI form factors to cancel that in the connected insertion (CI) [23,24], taking the $q^2 \to 0$ limit in Eq. (7) can lead to large systematic error. In view of this, we calculated the unnormalized $g_A^L(q^2) = g_A(q^2)/\kappa_A$ and the induced pseudoscalar form factor $h_A^L(q^2) = h_A(q^2)/\kappa_A$ with the 3-point to 2-point correlator summed ratio $R(q_i, q_j)$ [19]

$$R(q_i, q_j, \Delta t) \underset{\Delta t \gg 1}{\to} \text{const} + \Delta t \left[\frac{E_q + m_N}{2E_q} \frac{g_A(q^2)}{\kappa_A} \delta_{ij} - \frac{q_i q_j}{2E_q} \frac{h_A(q^2)}{\kappa_A} \right], \tag{14}$$

where i and j denote the directions of the axial current and the nucleon polarization. Here g_A and h_A are normalized form factors. Sandwiching the AWI between the nucleon states with finite momentum transfer, one obtains

$$2m_N g_A^{s(N)}(q^2) + q^2 h_A^{s(N)}(q^2) = 2m g_P^s(q^2) + 2m_N g_G(q^2). \tag{15}$$

With 18 data points for $R(q_i, q_j)$ for different q_i and six data points for $2m g_P^s(q^2)$ and $g_G(q^2)$ for six different $-q^2$, we fit Eqs. (14) and (15) to obtain $g_A^{s(N)}(q^2)$ [including $g_A^{s(N)}(0)$], $h_A^{s(N)}(q^2)$, and κ_A. Since it is a global fit with all the q^2 data included, this method does not require modeling the q^2 behavior with any assumed functional form.

The results for normalized $g_A^s(q^2)$, $h_A^s(q^2)$ are plotted in Fig. 3 as a function of $-q^2$. Also plotted is $g_A^{s(N)}(q^2) + \frac{q^2}{2m_N} h_A^{s(N)}(q^2)$ which is compared to $\frac{m}{m_N} g_P^s(q^2) + g_G(q^2)$ from the AWI in Eq. (15). We see that the agreement is good for the range of $-q^2$ except for the last point at $-q^2 = 0.207$ GeV^2 where there is a two-sigma difference.

From the fit, we obtain $g_A^s = \Delta s + \Delta\bar{s} = -0.0372(36)$ and $\kappa_A = 1.36(4)$ at the unitary point where $m_\pi = 330$ MeV. $\Delta s + \Delta\bar{s}$ and κ_A have been calculated this way for several valence quark masses in the nucleon while keeping the

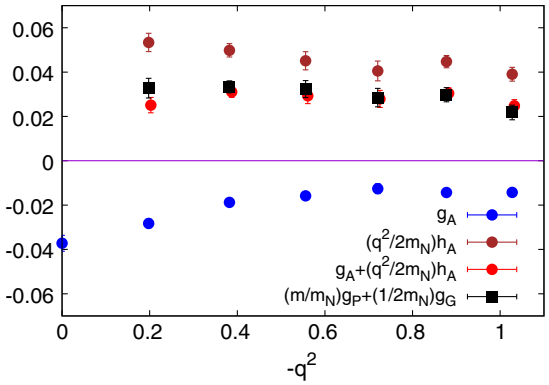

FIG. 3. The $-q^2$ dependence of the fitted normalized $g_A^s(q^2)$, $\frac{q^2}{2m_N}h_A^s(q^2)$ and their sum in comparison with $\frac{m}{m_N}g_P^s(q^2)+\frac{1}{2m_N}g_G(q^2)$. The latter is directly calculated. This is the case for the strange quark.

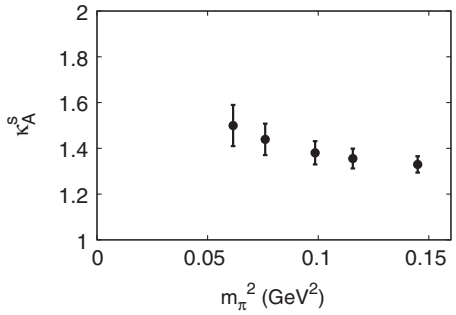

FIG. 4. The normalization factor κ_A as a function of valence m_π^2 while keeping the quark loop at the strange quark point.

quark loop at the strange quark point. The valence mass dependence of κ_A is plotted in Fig. 4. We see that κ_A is larger than 1, and becomes larger as the valence quark mass decreases.

The chiral behavior of $\Delta s+\Delta\bar{s}$ is plotted in Fig. 5 as a function of m_π^2 according to the valence quark mass. We see that the results are fairly linear in m_π^2. Thus we fit it linearly in m_π^2 with the form $A+B(m_\pi^2-m_{\pi,\mathrm{phys}}^2)$ where $m_{\pi,\mathrm{phys}}$ is the physical pion mass and obtain $\Delta s+\Delta\bar{s}=-0.0403(44)$ at

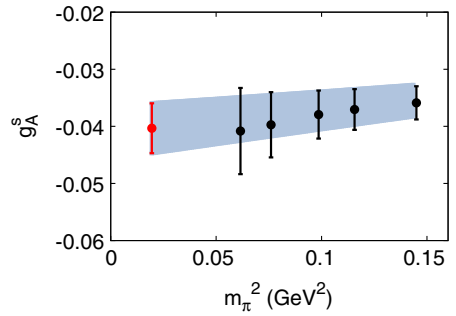

FIG. 5. Chiral extrapolation for the strange quark spin $\Delta s+\Delta\bar{s}$ as a function of m_π^2.

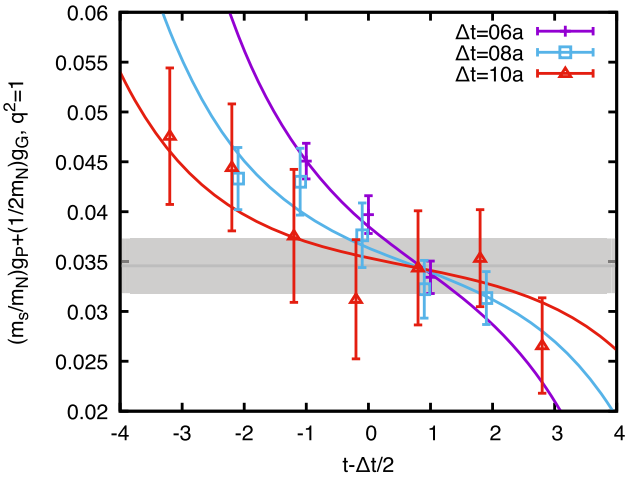

FIG. 6. The 3-pt-to-2-pt ratio for $\frac{m_s}{m_N}g_P^s(q^2)+\frac{1}{2m_N}g_G(q^2)$ at the smallest $q^2=-0.207$ GeV^2 as a function of $t-t_f/2$. The separations $\Delta t=t_f-t_i=6,\ 8,\ 10$ are shown with the data series. The lines on them are from two-state fit for the separate Δt. The grey band indicates the combined two-state and sum method fit.

the physical pion mass. This is shown in Fig. 5. The uncertainty estimated through the variance from several different fits by adding a $m_\pi^2\log(m_\pi^2/\Lambda^2)$ term, a m_π^3 term, or a m_π^4 term to the chiral extrapolation formula gives a systematic error of 0.0013.

In this work, we adopted the sum method to extract the matrix elements. To assess the excited state contamination, we use the combined two-state fit with the sum method used in the calculation of the πN and strange sigma terms [35], strange magnetic moment [36], and glue spin [37] for comparison for a few cases. We first plot in Fig. 6 the unsummed ratios in Eq. (13) for $\frac{m_s}{m_N}g_P^s(q^2)+\frac{1}{2m_N}g_G(q^2)$ at the smallest $q^2=-0.207$ GeV^2 as a function of $t-t_f/2$

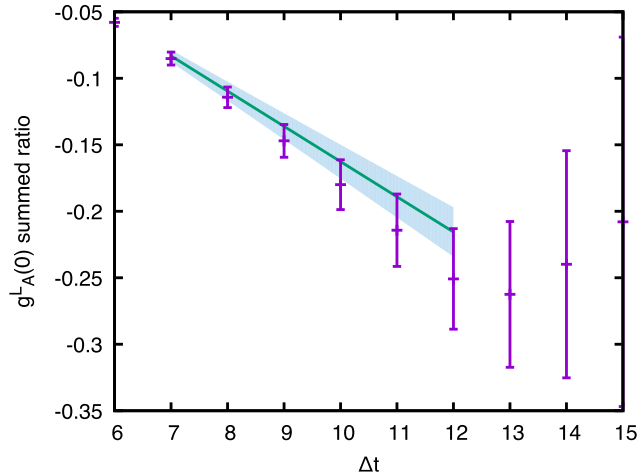

FIG. 7. The summed ratio as a function of Δt for the calculation of $g_A^L(0)$ which is extracted from the slope as in Eq. (13).

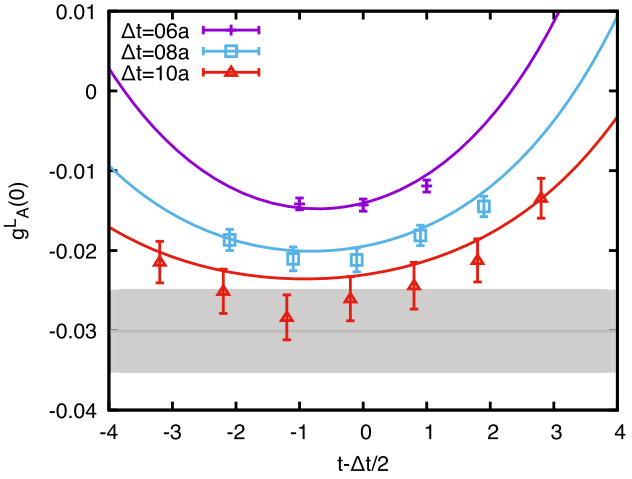

FIG. 8. The same as in Fig. 6 for the bare $g_A^L(0)$.

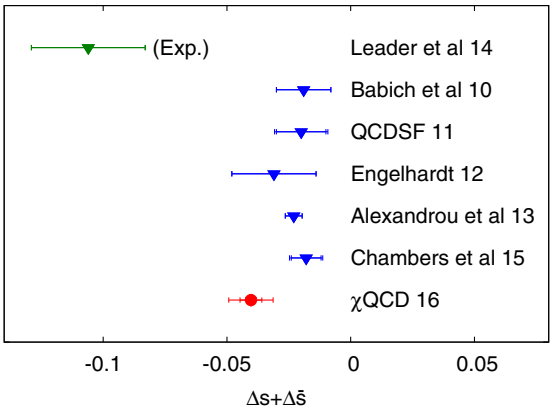

FIG. 9. A summary of the recent lattice QCD calculations of the strange quark spin $\Delta s + \Delta\bar{s}$ compared with the global fit of experiments. The blue triangles are lattice calculations from the axial vector current and the red circle is from the present work which uses the anomalous Ward identity.

for time separations $\Delta t = 6, 8, 10$ between the source and the sink. A combined two-state and sum method fit with these data produces a value of 0.035(3) which is consistent with the slope extracted using the sum method which is 0.033(4).

Similarly, we have done the comparison for $g_A^L(0)$. Plotted in Fig. 7 is the summed ratio of 3-pt-to-2-pt correlators as a function of Δt for the calculation of $g_A^L(0)$ which is extracted from the slope as is from Eq. (13). At the unitary point, we obtain $g_A^L(0) = -0.027(3)$. Also plotted in Fig. 8 are the unsummed ratios for $g_A(0)$ as a function of $t - t_f/2$ for time separations $\Delta t = 6, 8, 10$ between the source and the sink. A combined two-state and sum method fit with these data yields a value of $-0.030(5)$. While their errors bands overlap, this is about 10% larger than the results of the sum method fit. We shall take this 10% difference as a systematic error of the present work.

The total systematic error contains the renormalization uncertainty $|\delta g_A^s| \sim 0.0066$, the uncertainty of the chiral extrapolation of 0.0013, and uncertainty due to the excited state contamination of the sum method of 0.0040. We sum them up quadratically and obtain an overall systematic error of 0.0078.

We list our result in Fig. 9 together with other recent lattice results in comparison with the global fit value extracted from the DIS data [10,11]. The blue triangles are lattice calculations of the axial vector current matrix element and the red circle is from the present work based on the anomalous Ward identity.

We see that our result, although still more than two sigmas smaller than the recent analysis of the DIS data which finds the strange spin to be $-0.106(23)$ [11], is somewhat larger in magnitude than the other direct calculations of the axial-vector current [5–9]. This is mainly due to the fact that the normalization factor $\kappa_A \sim 1.36$, which is required to have the AWI satisfied in our calculation, is larger than that for the isovector axial-vector current which is 1.10 in our case. Presumably, a similarly larger κ_A exists for the other calculations using axial-vector currents which do not satisfy the AWI, but has not been taken into account.

IV. CONCLUSION

In summary, we have carried out a calculation of the strange and charm quark spin contributions to the spin of the nucleon with the help of the anomalous axial Ward identity. This is done using overlap fermions for the nucleon and the quark loop on $2+1$ flavor DWF, $24^3 \times 64$ configurations with light sea quarks corresponding to $m_\pi = 330$ MeV. Since the overlap fermion is used for the pseudoscalar term $2mP$ and the overlap Dirac operator is used for the local topological term, the normalized AWI also holds for the renormalized AWI to two-loop order. For the charm quark, we find that the $2mP$ term and the anomaly contributions almost cancel. For the strange quark, the $2mP$ term is somewhat smaller than that of the charm. Fitting the AWI at finite q^2 and the $g_A(q^2)$ and $h_A(q^2)$ form factors, we obtain the normalized $g_A^s(0)$. The normalization factor $\kappa_A \sim 1.36$ for the local axial-vector current is found to be larger than that for the isovector axial-vector current, which implies that it is affected by a large cutoff effect presumably due to the triangle anomaly. This will be clarified by future work using the conserved axial-vector current [38] for overlap fermions. After chiral extrapolation to the physical pion mass, we obtain $\Delta c + \Delta\bar{c} = -2.7(2.8) \times 10^{-4}$ which is consistent with zero, and $\Delta s + \Delta\bar{s} = -0.0403(44)(78)$ which is smaller in magnitude than that from the latest analysis of DIS data [10,11] by more than two sigmas. We plan to rerun the analysis on configurations with lighter sea quark masses to gauge the effect of this parameter on the results reported in this paper. In this work, we have identified the source for the negative spin contribution in the disconnected insertion of the light quarks

as due to the large and negative $2mP$ contribution which overcomes the positive anomaly contribution to give an overall negative $g_A^s(0)$. This is likely the cause for the smallness of the net quark spin in the nucleon. We will confirm this later with results on the u and d quarks from both the disconnected and connected insertions.

ACKNOWLEDGMENTS

We thank RBC and UKQCD for sharing the DWF gauge configurations that we used in the present work. This work is supported in part by the National Science Foundation of China (NSFC) under Project No. 11405178, the Youth Innovation Promotion Association of CAS (2015013), and the U.S. DOE Grant No. DE-SC0013065. A. A. is supported in part by the National Science Foundation CAREER Grant No. PHY-1151648 and by U.S. DOE Grant No. DE-FG02-95ER40907. This research used resources of the Oak Ridge Leadership Computing Facility at the Oak Ridge National Laboratory, which is supported by the Office of Science of the U.S. Department of Energy under Contract No. DE-AC05-00OR22725. This work also used the Extreme Science and Engineering Discovery Environment (XSEDE), which is supported by National Science Foundation Grant No. ACI-1053575.

[1] D. de Florian, R. Sassot, M. Stratmann, and W. Vogelsang, Extraction of spin-dependent parton densities and their uncertainties, Phys. Rev. D **80**, 034030 (2009).
[2] S. J. Dong, J.-F. Lagae, and K. F. Liu, Flavor Singlet g(A) from Lattice QCD, Phys. Rev. Lett. **75**, 2096 (1995).
[3] M. Fukugita, Y. Kuramashi, M. Okawa, and A. Ukawa, Proton Spin Structure from Lattice QCD, Phys. Rev. Lett. **75**, 2092 (1995).
[4] S. Güsken, P. Ueberholz, J. Viehoff, N. Eicker, T. Lippert, K. Schilling, A. Spitz, and T. Struckmann (TXL Collaboration), Flavor singlet axial vector coupling of the proton with dynamical Wilson fermions, Phys. Rev. D **59**, 114502 (1999).
[5] G. S. Bali *et al.* (QCDSF Collaboration), Strangeness Contribution to the Proton Spin from Lattice QCD, Phys. Rev. Lett. **108**, 222001 (2012).
[6] R. Babich, R. C. Brower, M. A. Clark, G. T. Fleming, J. C. Osborn, C. Rebbi, and D. Schaich, Exploring strange nucleon form factors on the lattice, Phys. Rev. D **85**, 054510 (2012).
[7] M. Engelhardt, Strange quark contributions to nucleon mass and spin from lattice QCD, Phys. Rev. D **86**, 114510 (2012).
[8] A. Abdel-Rehim, C. Alexandrou, M. Constantinou, V. Drach, K. Hadjiyiannakou, K. Jansen, G. Koutsou, and A. Vaquero, Disconnected quark loop contributions to nucleon observables in lattice QCD, Phys. Rev. D **89**, 034501 (2014).
[9] A. J. Chambers *et al.*, Disconnected contributions to the spin of the nucleon, Phys. Rev. D **92**, 114517 (2015).
[10] E. Leader, A. V. Sidorov, and D. B. Stamenov, New analysis concerning the strange quark polarization puzzle, Phys. Rev. D **91**, 054017 (2015).
[11] D. Stamenov and E. Leader (private communication).
[12] L. H. Karsten and J. Smit, Lattice fermions: Species doubling, chiral invariance, and the triangle anomaly, Nucl. Phys. **B183**, 103 (1981).
[13] J. F. Lagae and K. F. Liu, Finite mass corrections for sea quark matrix elements on the lattice, Phys. Rev. D **52**, 4042 (1995).
[14] H. Neuberger, Exactly massless quarks on the lattice, Phys. Lett. B **417**, 141 (1998).
[15] P. Hasenfratz, S. Hauswirth, T. Jorg, F. Niedermayer, and K. Holland, Testing the fixed point QCD action and the construction of chiral currents, Nucl. Phys. **B643**, 280 (2002).
[16] T. Draper *et al.*, Locality and scaling of quenched overlap fermions, *Proc. Sci.*, LAT2005 (2006) 120 [arXiv:hep-lat/0510075].
[17] Y. Kikukawa and A. Yamada, Weak coupling expansion of massless QCD with a Ginsparg-Wilson fermion and axial U(1) anomaly, Phys. Lett. B **448**, 265 (1999); D. H. Adams, Axial anomaly and topological charge in lattice gauge theory with overlap Dirac operator, Ann. Phys. (N.Y.) **296**, 131 (2002); K. Fujikawa, A continuum limit of the chiral Jacobian in lattice gauge theory, Nucl. Phys. **B546**, 480 (1999); H. Suzuki, Simple evaluation of chiral Jacobian with overlap Dirac operator, Prog. Theor. Phys. **102**, 141 (1999).
[18] K. F. Liu, S. J. Dong, T. Draper, and W. Wilcox, Pi N N and Pseudoscalar Form-Factors from Lattice QCD, Phys. Rev. Lett. **74**, 2172 (1995).
[19] The typical form for the ratio in Eq. (14) can be found in M. Deka, T. Doi, Y. B. Yang, B. Chakraborty, S. J. Dong, T. Draper, M. Glatzmaier, M. Gong, H. W. Lin, K. F. Liu, D. Mankame, N. Mathur, and T. Streuer, Lattice study of quark and glue momenta and angular momenta in the nucleon, Phys. Rev. D **91**, 014505 (2015).
[20] M. Luscher, S. Sint, R. Sommer, and H. Wittig, Non-perturbative determination of the axial current normalization constant in O(a) improved lattice QCD, Nucl. Phys. **B491**, 344 (1997).
[21] J. E. Mandula, A Lattice Simulation of the Anomalous Gluon Contribution to the Proton Spin, Phys. Rev. Lett. **65**, 1403 (1990).
[22] R. Altmeyer, M. Gockeler, R. Horsley, E. Laermann, and G. Schierholz, The axial baryonic charge and the spin content of the nucleon: A lattice investigation, Phys. Rev. D **49**, R3087 (1994).

[23] K. F. Liu, Flavor singlet axial charge of the nucleon and anomalous Ward identity, Phys. Lett. B **281**, 141 (1992).
[24] K. F. Liu, Comments on lattice calculations of proton spin components, arXiv:hep-lat/9510046.
[25] D. Espriu and R. Tarrach, Renormalization of the axial anomaly operators, Z. Phys. C **16**, 77 (1982).
[26] For lattice perturbation theory, see for example, S. Capitani, Lattice perturbation theory, Phys. Rep. **382**, 113 (2003).
[27] Y. Aoki *et al.* (RBC and UKQCD Collaborations), Continuum limit physics from $2+1$ flavor domain wall QCD, Phys. Rev. D **83**, 074508 (2011).
[28] M. Lujan, A. Alexandru, Y. Chen, T. Draper, W. Freeman, M. Gong, F. X. Lee, A. Li, K. F. Liu, and N. Mathur, The Δ_{mix} parameter in the overlap on domain-wall mixed action, Phys. Rev. D **86**, 014501 (2012).
[29] M. Gong *et al.* (χQCD Collaboration), Strangeness and charmness content of the nucleon from overlap fermions on $2+1$-flavor domain-wall fermion configurations, Phys. Rev. D **88**, 014503 (2013).
[30] Y. B. Yang, Y. Chen, A. Alexandru, S. J. Dong, T. Draper, M. Gong, F. X. Lee, A. Li, K. F. Liu, Z. Liu, and M. Lujan, Charm and strange quark masses and f_{D_s} from overlap fermions, Phys. Rev. D **92**, 034517 (2015).
[31] L. Maiani, G. Martinelli, M. L. Paciello, and B. Taglienti, Scalar densities and baryon mass differences in lattice QCD with Wilson fermions, Nucl. Phys. **B293**, 420 (1987).
[32] M. Deka, T. Streuer, T. Doi, S. J. Dong, T. Draper, K. F. Liu, N. Mathur, and A. W. Thomas, Moments of nucleon's parton distribution for the sea and valence quarks from lattice QCD, Phys. Rev. D **79**, 094502 (2009).
[33] A. Li *et al.* (χQCD Collaboration), Overlap valence on $2+1$ flavor domain wall fermion configurations with deflation and low-mode substitution, Phys. Rev. D **82**, 114501 (2010).
[34] M. Franz, M. V. Polyakov, and K. Goeke, Heavy quark mass expansion and intrinsic charm in light hadrons, Phys. Rev. D **62**, 074024 (2000).
[35] Y.-B. Yang, A. Alexandru, T. Draper, J. Liang, and K.-F. Liu (χQCD Collaboration), πN and strangeness sigma terms at the physical point with chiral fermions, Phys. Rev. D **94**, 054503 (2016).
[36] R. S. Sufian, Y. B. Yang, A. Alexandru, T. Draper, K. F. Liu, and J. Liang, Strange Quark Magnetic Moment of the Nucleon at Physical Point, Phys. Rev. Lett. **118**, 042001 (2017).
[37] Y. B. Yang, R. S. Sufian, A. Alexandru, T. Draper, M. J. Glatzmaier, K. F. Liu, and Y. Zhao, Glue Spin and Helicity in Proton from Lattice QCD, Phys. Rev. Lett. **118**, 102001 (2017).
[38] P. Hasenfratz, V. Laliena, and F. Niedermayer, The index theorem in QCD with a finite cutoff, Phys. Lett. B **427**, 125 (1998).